The ground state of an $S = 1/2$ distorted diamond chain - a model of $Cu_3Cl_6(H_2O)_2 \cdot 2H_8C_4SO_2$

1999 J. Phys.: Condens. Matter 11 10485

(http://iopscience.iop.org/0953-8984/11/50/336)

J. Phys.: Condens. Matter **11** (1999) 10485–10498. Printed in the UK PII: S0953-8984(99)06479-6

The ground state of an $S = 1/2$ distorted diamond chain—a model of $Cu_3Cl_6(H_2O)_2{\cdot}2H_8C_4SO_2$

Kiyomi Okamoto†, Taskashi Tonegawa‡, Yutaka Takahashi§ and Makoto Kaburagi‖

† Department of Physics, Tokyo Institute of Technology, Oh-Okayama, Meguro-ku, Tokyo 152-8551, Japan
‡ Department of Physics, Faculty of Science, Kobe University, Rokkodai, Kobe 657-8501, Japan
§ Division of Physics, Graduate School of Science and Technology, Kobe University, Rokkodai, Kobe 657-8501, Japan
‖ Department of Informatics, Faculty of Cross-Cultural Studies, Kobe University, Tsurukabuto, Kobe 657-8501, Japan

Received 30 July 1999, in final form 30 September 1999

Abstract. We study the ground state of the model Hamiltonian of the trimerized $S = 1/2$ quantum Heisenberg chain $Cu_3Cl_6(H_2O)_2{\cdot}2H_8C_4SO_2$ in which a non-magnetic ground state was observed recently. This model consists of stacked trimers and has three kinds of coupling constant describing the couplings between spins: the intra-trimer coupling constant J_1 and the inter-trimer coupling constants J_2 and J_3. All of these constants are assumed to be antiferromagnetic. By use of an analytical method and physical considerations, we show that there are three phases on the $\tilde{J}_2$–$\tilde{J}_3$ plane ($\tilde{J}_2 \equiv J_2/J_1$, $\tilde{J}_3 \equiv J_3/J_1$): the dimer phase, the spin-fluid phase and the ferrimagnetic phase. The dimer phase is caused by the frustration effect. In the dimer phase, there exists an excitation gap between the twofold-degenerate ground state and the first excited state, which explains the non-magnetic ground state observed in $Cu_3Cl_6(H_2O)_2{\cdot}2H_8C_4SO_2$. We also obtain the phase diagram on the $\tilde{J}_2$–$\tilde{J}_3$ plane from the numerical diagonalization data for finite systems by use of the Lanczos algorithm.

1. Introduction

In recent years low-dimensional quantum spin systems have attracted a great deal of attention. Very recently, Ishii *et al* [1] have experimentally studied a trimerized quantum spin chain $Cu_3Cl_6(H_2O)_2{\cdot}2H_8C_4SO_2$. They have measured the temperature dependence of the spin susceptibility, and the magnetization curve at low temperatures. Their results show that the magnetic susceptibility χ behaves as $\chi \to 0$ at $T \to 0$ and there exists a critical magnetic field where the magnetization rises up from zero. Thus they have concluded that the ground state of this substance is non-magnetic. From the result of a structure-analysis experiment [2], the chain is known to be composed of stacked $S = 1/2$ Cu^{2+} trimers and separated from other chains by large molecules, $H_8C_4SO_2$. Therefore this substance is thought to be well modelled by independent chains of stacked trimers and Ishii *et al* have proposed the model shown in figure 1 [1].

In this paper we call this model the 'distorted diamond (DD) chain model'. The

0953-8984/99/5010485+14$30.00

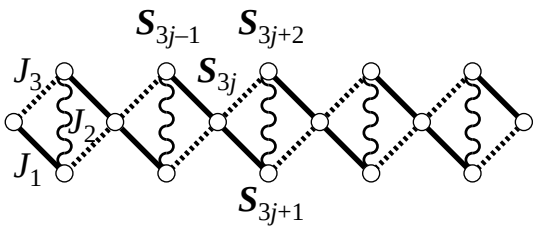

Figure 1. A sketch of the model of $Cu_3Cl_6(H_2O)_2{\cdot}2H_8C_4SO_2$. Solid lines denote the intra-trimer coupling J_1, wavy lines the inter-trimer coupling J_2 and dotted lines the inter-trimer coupling J_3.

Hamiltonian of this model is written as

$$H = J_1 \sum_j (\boldsymbol{S}_{3j-1} \cdot \boldsymbol{S}_{3j} + \boldsymbol{S}_{3j} \cdot \boldsymbol{S}_{3j+1}) + J_2 \sum_j \boldsymbol{S}_{3j+1} \cdot \boldsymbol{S}_{3j+2} + J_3 \sum_j (\boldsymbol{S}_{3j-2} \cdot \boldsymbol{S}_{3j} + \boldsymbol{S}_{3j} \cdot \boldsymbol{S}_{3j+2}) \tag{1}$$

where three spins $\boldsymbol{S}_{3j-1}$, $\boldsymbol{S}_{3j}$ and $\boldsymbol{S}_{3j+1}$ form a trimer. All the coupling constants are supposed to be positive (antiferromagnetic). Although it is thought that $J_1 > J_2, J_3$ in $Cu_3Cl_6(H_2O)_2{\cdot}2H_8C_4SO_2$ because of its structure, we do not restrict ourselves to this case. Hereafter we take J_1 as the energy unit and set $\tilde{J}_2 \equiv J_2/J_1$ and $\tilde{J}_3 \equiv J_3/J_1$. We note that the point $(\tilde{J}_2, \tilde{J}_3)$ is equivalent to the point $(\tilde{J}_2/\tilde{J}_3, 1/\tilde{J}_3)$ on interchanging the roles of J_1 and J_3.

If we transform the Hamiltonian (1) into the fermion representation through the Jordan–Wigner transformation, we can see that the fermionic band gap exists at $M = M_s/3$ but not at $M = 0$, where M_s is the saturation magnetization [3,4]. Thus the trimerization itself cannot be the direct reason for the non-magnetic ground state. This can also be explained by considering the necessary condition for the appearance of magnetization plateau proposed by Oshikawa, Yamanaka and Affleck [5],

$$n(S - \langle m \rangle) = \text{integer} \tag{2}$$

where n is the periodicity of the ground-state wave function, S the magnitude of the spins and $\langle m \rangle$ the average magnetization per spin in the plateau. The periodicity of the Hamiltonian (1) itself is 3. We see that $n = 3$ does not satisfy condition (2) with $S = 1/2$ and $\langle m \rangle = 0$. Then, if the present model is applicable to $Cu_3Cl_6(H_2O)_2{\cdot}2H_8C_4SO_2$, its ground-state wave function should have periodicity with at least $n = 6$ due to the spontaneous symmetry breaking. In this paper, we explain why the non-magnetic ground state is realized and derive the ground-state phase diagram on the $\tilde{J}_2$–$\tilde{J}_3$ plane.

The $J_1 = J_3$ case of the present model was named the 'diamond chain' and investigated by Takano, Kubo and Sakamoto (TKS) [6]. They concluded that the ground state of the diamond chain is composed of three phases: the ferrimagnetic phase ($M = M_s/3$) for $\tilde{J}_2 < 0.909$, the tetramer–dimer phase for $0.909 < \tilde{J}_2 < 2$ and the dimer–monomer phase for $\tilde{J}_2 > 2$. The relation between the present model and TKS's model will be discussed later.

This paper is organized as follows. In section 2, we explain the mechanism for the non-magnetic ground state by use of an analytical method and physical consideration. In section 3, we obtain the phase diagram from the numerical data for the diagonalization of the Hamiltonian (1) for finite systems by use of the Lanczos algorithm. The last section is devoted to discussion.

2. Analytical and physical approach

We consider three special cases at first. When $\tilde{J}_2 = 1$ and $\tilde{J}_3 = 0$, the present model is reduced to the simple $S = 1/2$ chain with nearest-neighbour interactions, the ground state of which is the spin-fluid (SF) state, as is well known. In the case of $\tilde{J}_2 = 0$, the ground state may be ferrimagnetic ($M = M_s/3$), because the state with $\boldsymbol{S}_{3j} = \downarrow$ and $\boldsymbol{S}_{3j\pm1} = \uparrow$ is the classical ground state. At the point $\tilde{J}_2 = \tilde{J}_3 = 0$, the chain is truncated into an array of independent trimers.

Next, let us consider the $\tilde{J}_2 = 1$ case. If we re-draw the model in the single-chain form as in figure 2, we see this is closely related to the next-nearest-neighbour (NNN) interaction model in figure 3. In fact, the model of figure 2 is obtained from that of figure 3 by removing one NNN interaction of every three NNN interactions. The important point is that every spin feels the frustration.

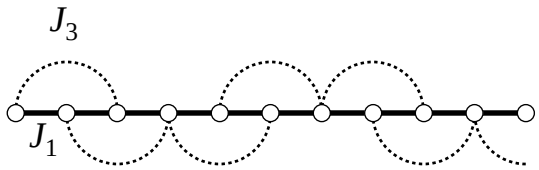

Figure 2. The present model in the $\tilde{J}_2 = 1$ case in the linear chain form.

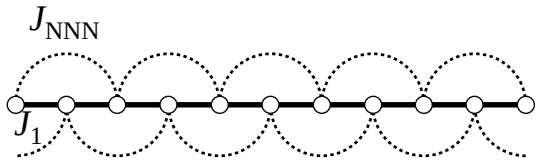

Figure 3. The next-nearest-neighbour (NNN) interaction model.

The NNN interaction model is one of the most important models having frustration and is extensively studied [7–15]. When $\tilde{J}_{\mathrm{NNN}} \equiv J_{\mathrm{NNN}}/J_1 = 0.5$, the ground state of the NNN interaction model is an array of independent singlet dimers, where the translational symmetry under translation by one spin spacing is spontaneously broken [7, 8]. Then there should exist a critical point of the ground-state phase transition between the spin-fluid (SF) state and the dimer state. Okamoto and Nomura [12] numerically determined this SF–dimer critical point, $\tilde{J}_{\mathrm{NNN}}^{(\mathrm{cr})} = 0.2411$.

Since the model of figure 2 is very similar to that of figure 3, as stated, the SF–dimer transition may occur also in the model of figure 2 when $\tilde{J}_2$ is increased. This can be confirmed by the bosonization technique in the following way. The effective Hamilton of the model of figure 3 in the continuum limit is written as [9, 11, 12, 14, 15]

$$H = \frac{1}{2\pi}\int \mathrm{d}x \left[v_s K (\pi \Pi)^2 + \frac{v_s}{K}\left(\frac{\partial \phi}{\partial x}\right)^2 \right] + \frac{y_\phi v_s}{2\pi}\int \mathrm{d}x \ \cos\sqrt{2}\phi \tag{3}$$

where v_s is the spin-wave velocity and K the quantum parameter which governs the algebraic decay of the spin-correlation functions:

$$\langle S_0^z S_r^z \rangle \sim r^{-K} \qquad \langle S_0^+ S_r^- \rangle \sim r^{-1/K} \tag{4}$$

in the SF state. Due to the isotropic nature of our model, the renormalized value of K should be $K = 1$. The variables $\phi(x)$ and $\Pi(x)$ are mutually conjugate:

$$[\phi(x), \Pi(x')] = \mathrm{i}\delta(x - x'). \tag{5}$$

The coefficient of the cosine term, y_ϕ in equation (3), is

$$y_\phi \propto \Delta - 3\tilde{J}_{\mathrm{NNN}} \tag{6}$$

where Δ is the XXZ anisotropy defined by $J^z/J^\perp$ which is equal to unity in our isotropic model. For the model of figure 2, we can obtain the effective Hamiltonian of the same form as (3), but with

$$y_\phi \propto \Delta - 2\tilde{J}_3. \tag{7}$$

We note that the expressions (6) and (7) are valid only in the lowest order of Δ, $\tilde{J}_{\mathrm{NNN}}$ and $\tilde{J}_3$. Since we take the continuum limit in the course of deriving the effective Hamiltonian, the difference between the two models appears as the difference in the expression of y_ϕ. We note that the spin-wave velocities v_{s} are slightly different in the two models, but this does not bring about any major effect. Thus we can conclude that the model of figure 2 also shows the SF–dimer phase transition. Since $3\tilde{J}_{\mathrm{NNN}}$ in equation (6) is replaced by $2\tilde{J}_3$ in equation (7), the critical value $\tilde{J}_3^{(\mathrm{cr})}$ is naively obtained by letting $3\tilde{J}_{\mathrm{NNN}}^{(\mathrm{cr})} = 2\tilde{J}_3^{(\mathrm{cr})}$, which leads to $\tilde{J}_3^{(\mathrm{cr})} \simeq 0.36$ on using $\tilde{J}_{\mathrm{NNN}}^{(\mathrm{cr})} = 0.2411$. In fact, as shown in section 4, the numerical result is $\tilde{J}_3^{(\mathrm{cr})} \simeq 0.354$. The dimer ground-state wave function in the model of figure 2 is twofold degenerate with periodicity $n = 6$ and is shown in figure 4.

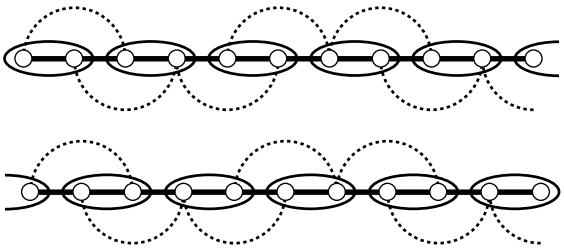

Figure 4. Dimer configurations in the ground state of the DD chain model with $\tilde{J}_2 = 1$ in the single-chain form. Two spins in an ellipse form a singlet dimer pair.

When $\tilde{J}_2 \neq 1$, we have to include the trimerization effects in the effective Hamiltonian. However, in the $M = 0$ subspace, the trimerization does not lead to a mass-generating term such as the cosine term in equation (3), although it slightly modifies the spin-wave velocity v_{s}. Then, as long as the trimerization is not so large (not so far from the $\tilde{J}_2 = 1$ line), the DD chain model also exhibits the SF–dimer phase transition. The dimer configuration of the DD chain model is easily found by tracing back the model mapping, which is shown in figure 5. This ground-state wave function is also twofold degenerate with periodicity $n = 6$.

Here we summarize the critical properties of the SF–dimer transition using the effective Hamiltonian (3) having the sine–Gordon form. The renormalization group calculation leads to

$$\frac{\mathrm{d}y_0(L)}{\mathrm{d}\ln L} = -y_\phi(L)^2 \qquad \frac{\mathrm{d}y_\phi(L)}{\mathrm{d}\ln L} = -y_0(L)y_\phi(L) \tag{8}$$

where L is an infrared cut-off and

$$y_0 \propto K - 1 \tag{9}$$

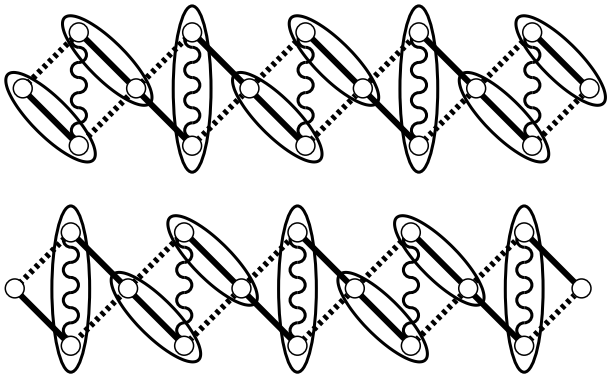

Figure 5. Dimer configurations in the ground state of the DD chain model. Two spins in an ellipse form a singlet dimer pair.

The flow diagram of this is shown in figure 6, from which we see that the SF–dimer transition is of the Berezinskii–Kosterlitz–Thouless type, as is well known. Since our model is isotropic, the renormalized value of K should be equal to unity, as already stated. Then, when the system is in the SF state, the starting point of the renormalization lies on the SF–Néel boundary line which flows into the origin where $K = 1$, and moves along the route A $\rightarrow$ B $\rightarrow$ C, as $\tilde{J}_2$ increases. Finally the SF–dimer transition takes place when the starting point arrives at the origin. In the SF state, $y_\phi(L) = -y_0(L)$ in equation (8), resulting in

$$y_0(L) = \frac{y_0^{(0)}}{y_0^{(0)} \ln(L/L_0) + 1} \tag{10}$$

where $y_0^{(0)}$ is the bare value of $y_0(L)$ and L_0 is the cut-off length. Then, there appear logarithmic corrections in various physical quantities at every point in the SF region in our isotropic (i.e., $SU(2)$-symmetric) model. At the SF–dimer critical point (origin O), on the other hand, the

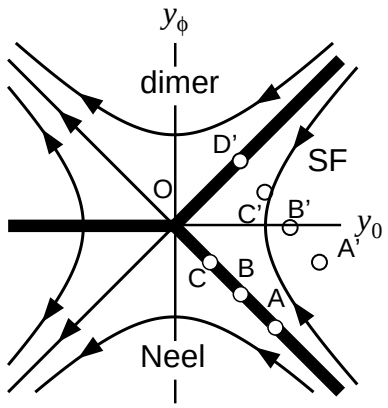

Figure 6. The renormalization flow of the effective Hamiltonian (3). The phase boundaries are shown by thick lines. In our isotropic case, the starting point of the renormalization lies on the SF–Néel boundary line. As $\tilde{J}_2$ increases, the starting point moves as A $\rightarrow$ B $\rightarrow$ C $\rightarrow$ O. If the system has the XXZ symmetry with $\Delta \equiv J^z/J^\perp < 1$, the starting point of the renormalization moves as A$'$ $\rightarrow$ B$'$ $\rightarrow$ C$'$ $\rightarrow$ D$'$.

logarithmic corrections vanish because $y_0 = y_\phi = 0$. This is very much peculiar to the isotropic case. Since the SF–dimer transition occurs at $y_\phi = 0$, one may think that the SF–dimer critical point can be obtained from equations (6) or (7). However, as stated, expressions (6) and (7) are valid only in the lowest order of Δ, $\tilde{J}_{\rm NNN}$ and $\tilde{J}_3$, although the critical properties are well expressed by the effective Hamiltonian. Then numerical calculation is needed for determining the SF–dimer critical point even in the case of $\tilde{J}_2 = 1$.

If the model has the XXZ symmetry (no longer isotropic) with $\Delta \equiv J^z/J^\perp < 1$, the starting point of the renormalization moves as $\mathrm{A}' \to \mathrm{B}' \to \mathrm{C}' \to \mathrm{D}'$ as $\tilde{J}_2$ increases. When the starting point arrives at D′, the SF–dimer transition occurs. Then, in the XXZ-symmetric case, the logarithmic corrections exist only at the SF–dimer critical point, and do not exist in the SF region.

3. Numerical result

To confirm the consideration in section 2 and to obtain the ground-state phase diagram on the $\tilde{J}_2$–$\tilde{J}_3$ plane, we performed the numerical diagonalization for finite systems for $N = 6, 12, 18, 24$ by use of the Lanczos algorithm under periodic boundary conditions. It is very easy to distinguish whether the ground state is ferrimagnetic ($M = M_{\rm s}/3$) or $M = 0$ from the numerical data. However, it is difficult to detect the SF–dimer critical point from the numerical data, because this transition is of the Berezinskii–Kosterlitz–Thouless type [9, 12] with pathological critical behaviour. Okamoto and Nomura (ON) [12] developed a method by use of which the SF–dimer critical point of the $S = 1/2$ NNN interaction model of figure 3 can be successfully determined from the numerical data for the energy gaps. Let us explain this method, focusing on its physical meaning. In usual cases, the ground state is unique (not twofold degenerate) in finite systems, except for the special cases such as the Ising model and the Majumdar–Ghosh model [7, 8]. How is the twofold-degenerate ground state realized in infinite systems? The energy gap of a low-lying excited state of finite systems rapidly decreases as the system size N increases, and is finally degenerate to the ground state as $N \to \infty$. Then the linear combination of the ground state and the above-mentioned excited state results in the twofold-degenerate ground state of the infinite systems. In our case, the ground state of finite systems has the property $S_{\rm tot} = 0$ as long as it lies in the $M = 0$ subspace (i.e., except for the ferrimagnetic case). The twofold-degenerate dimer state of infinite systems also has the property $S_{\rm tot} = 0$. Then the above-mentioned excited state should also have $S_{\rm tot} = 0$, because of the law of the addition of the angular momentum. Then we can conclude that the lowest excitation in finite systems has $S_{\rm tot} = 0$ in the dimer region. In the SF region, on the other hand, the lowest excitation should be of the spin-wave type with $S^z_{\rm tot} = \pm 1$ (the one-magnon state). In the present case, the excitation with the same energy exists in the $S^z_{\rm tot} = 0$ subspace due to the isotropic nature. This means that the system has threefold-degenerate lowest excitation with $S_{\rm tot} = 1$, when it lies in the SF region.

From the above physical consideration, we can write down the following criteria:

$$\begin{aligned} &\Delta E_{\rm ss}(N) < \Delta E_{\rm st}(N) \Longleftrightarrow \text{dimer state} \\ &\Delta E_{\rm ss}(N) > \Delta E_{\rm st}(N) \Longleftrightarrow \text{spin-fluid state} \end{aligned} \tag{11}$$

where $\Delta E_{\rm ss}(N)$ and $\Delta E_{\rm st}(N)$ are the singlet–singlet energy gap and singlet–triplet energy gap for a finite-size system with N spins, defined by

$$\Delta E_{\rm ss}(N) \equiv E_1(N, S^{(\rm tot)} = 0) - E_{\rm g}(N) \tag{12}$$

$$\Delta E_{\rm ss}(N) \equiv E_0(N, S^{(\rm tot)} = 1) - E_{\rm g}(N) \tag{13}$$

respectively. Here $E_0(N, S^{(\mathrm{tot})})$ and $E_1(N, S^{(\mathrm{tot})})$ are the lowest and second-lowest energies in the subspace with $S^{(\mathrm{tot})} = 0$, respectively, and $E_\mathrm{g} = E_0(S^{(\mathrm{tot})} = 0)$. These criteria can be obtained also by use of the effective-Hamiltonian representation, the renormalization group method and the conformal field theory [12, 14, 15].

Figure 7 shows the crossing between $S_\mathrm{tot} = 0$ and $S_\mathrm{tot} = 1$ excitations when $\tilde{J}_2 = 0.8$ and $N = 18$. By use of the interpolation, we see that the crossing point is $\tilde{J}_3^{(\mathrm{cr})}(N = 18) = 0.375\,263$. We can obtain the SF–dimer critical point of the infinite system by extrapolating $\tilde{J}_3^{(\mathrm{cr})}(N)$ to $N \to \infty$. The finite-size dependence of $\tilde{J}_3^{(\mathrm{cr})}(N)$ has the form

$$\tilde{J}_3^{(\mathrm{cr})}(N) = \tilde{J}_3^{(\mathrm{cr})}(\infty) + (\mathrm{constant}/N^2) \tag{14}$$

due to the existence of the irrelevant fields, as was discussed in [12, 14, 15]. Figure 8 shows the extrapolation of $\tilde{J}_3^{(\mathrm{cr})}(N)$ to $N \to \infty$ in the case of $\tilde{J}_2 = 0.8$, resulting in $\tilde{J}_3^{\mathrm{cr}} = 0.352 \pm 0.001$.

By sweeping parameters, we finally obtain the phase diagram on the $\tilde{J}_2$–$\tilde{J}_3$ plane. The result is shown in figure 9. We note that the point $(\tilde{J}_2, \tilde{J}_3)$ is equivalent to the point $(\tilde{J}_2/\tilde{J}_3, 1/\tilde{J}_3)$ on interchanging the role of J_1 and J_3, as already stated in section 1.

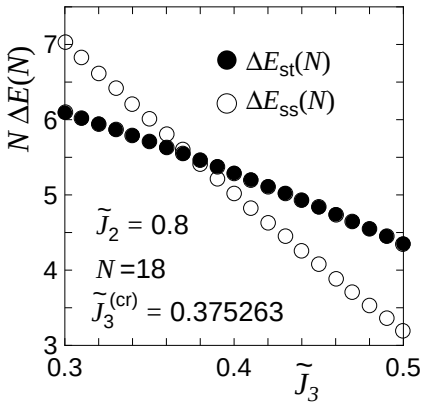

Figure 7. Level crossing between $\Delta E_{\mathrm{ss}}(N)$ and $\Delta E_{\mathrm{ss}}(N)$ when $\tilde{J}_2 = 0.8$ and $N = 18$. From the crossing point, we obtain $\tilde{J}_3^{(\mathrm{cr})}(N = 18) = 0.375\,263$.

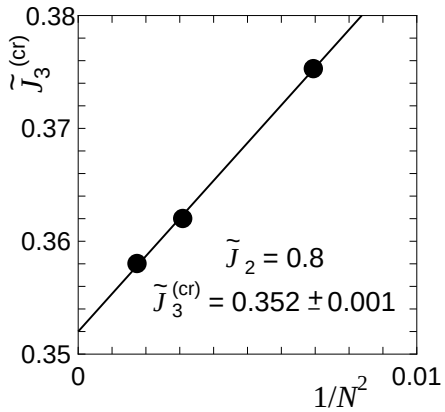

Figure 8. The extrapolation of $\tilde{J}_3^{(\mathrm{cr})}$ to $N \to \infty$ in the $\tilde{J}_2 = 0.8$ case. From this, we see that $\tilde{J}_3^{(\mathrm{cr})} = 0.352 \pm 0.001$.

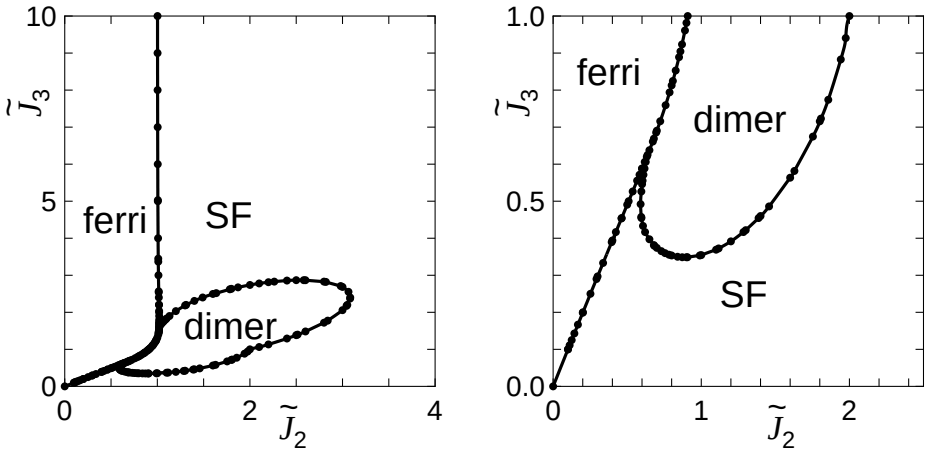

Figure 9. The phase diagram of the DD chain model. The estimated errors in the critical values are less than 0.001. The $\tilde{J}_3 = 1$ case is reduced to the model of Takano *et al* (see section 4).

4. Discussion

In section 2, we have stated that the ground-state quantum phase transition of the DD chain model (the present model) has the same universality class as that of the NNN model (figure 3). We have confirmed this analytically by use of the effective-Hamiltonian representation. Here we also confirm this by a numerical method.

Let us consider the model of figure 10 which interpolates between the DD chain model with $\tilde{J}_2 = 1$ (figure 2) and the NNN interaction model (figure 3). When $J_4/J_3 = 0$ the interpolation model is reduced to the DD chain model with $\tilde{J}_2 = 1$, and when $J_4/J_3 = 1$ to the NNN interaction model. Figure 11 shows the level crossings between $\Delta_{\rm st}(N)$ and $\Delta_{\rm ss}(N)$ for the $J_4/J_3 = 0$ and $J_4/J_3 = 1$ cases. The behaviour of the level crossing is essentially the same when the parameter J_4/J_3 runs from $J_4/J_3 = 0$ to $J_4/J_3 = 1$, as can be seen from figure 11. Furthermore, any other excitations cross them between $J_4/J_3 = 0$ to $J_4/J_3 = 1$. Figure 12 shows the SF–dimer critical point $J_3^{\rm cr}$ of the interpolation model, in which the critical point smoothly changes. Thus we can safely conclude that the ground-state quantum phase transition of the DD chain model (the present model) has the same universality class as that of the NNN interaction model (figure 3). The DD chain model with $\tilde{J}_2 = 1$ is obtained from the NNN interaction model by removing one NNN interaction in every three NNN interactions, as already stated. Instead of removal, a similar (but not exact) effect may be realized by decreasing the strength of the NNN interaction to $2/3$ of the original strength. If this is the case, the SF–dimer critical point of the DD chain model with $\tilde{J}_2 = 1$ is $3/2$ of that of the NNN

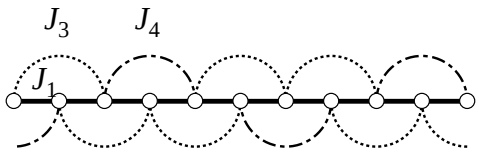

Figure 10. The model interpolating between the DD chain model with $\tilde{J}_2 = 1$ and the NNN interaction model. Solid lines denote J_1, dotted lines J_3 and dot–dashed lines J_4.

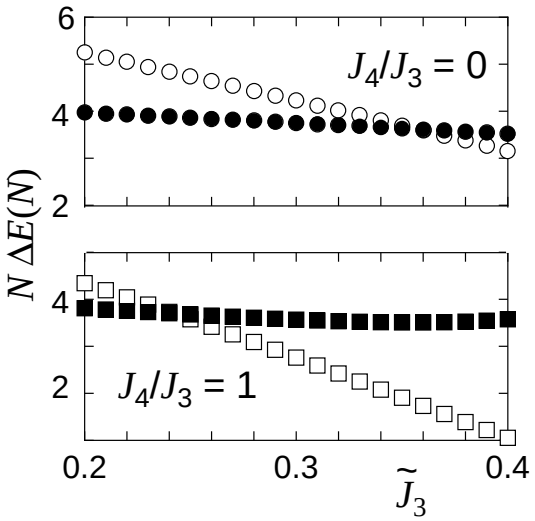

Figure 11. Level crossing of the interpolation model when $J_4/J_3 = 0$ and $J_4/J_3 = 1$ for $N = 18$. Closed circles and squares represent $\Delta_{\rm st}(N)$, and open circles and squares $\Delta_{\rm ss}(N)$.

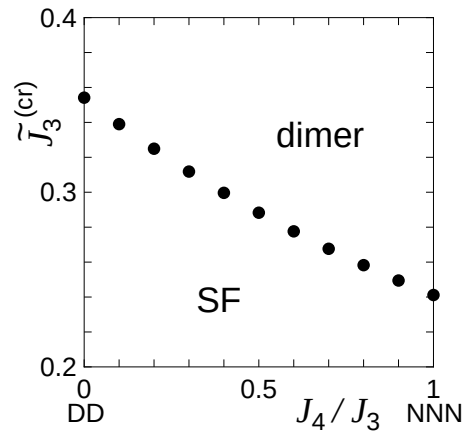

Figure 12. The SF–dimer critical points of the model interpolating between the DD chain model with $\tilde{J}_2 = 1$ and the NNN interaction model.

interaction model, which results in $\tilde{J}_3^{(\rm cr)} = (3/2) \times 0.2411 \simeq 0.36$. This semiqualitatively explains our numerical result $\tilde{J}_3^{(\rm cr)} = 0.354 \pm 0.001$ when $\tilde{J}_2 = 1$. This fact also appears in equations (6) and (7).

Takano, Kubo and Sakamoto (TKS) [6] investigated the $J_3 = J_1$ case of the present DD chain model (see figure 13(a)). They concluded that the ground state of their model is composed of three phases. The ferrimagnetic phase ($M = M_{\rm s}/3$) appears when $\tilde{J}_2 < 0.909$. In the tetramer–dimer (TD) phase, which appears when $0.909 < \tilde{J}_2 < 2$, the state is exactly the regular array of tetramers and dimers as shown in figure 13(b). Figure 13(c) shows the dimer–monomer (DM) state, appearing when $\tilde{J}_2 > 2$, which is composed of the regular array of singlet dimers and free spins. Because of the free spins, the DM state is macroscopically degenerate.

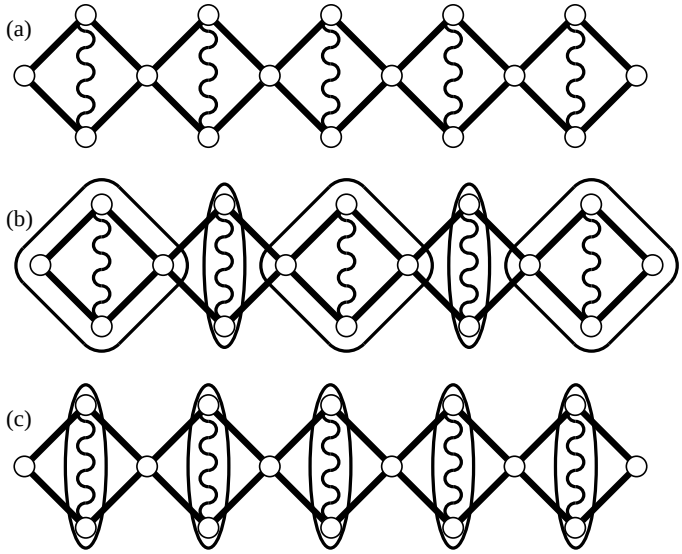

Figure 13. (a) The model of Takano, Kubo and Sakamoto. (b) The tetramer–dimer (TD) state. The rectangles represent tetramers and the ellipses singlet dimers. (c) The dimer–monomer (DM) state.

Let us discuss the relation between our model and TKS's model. In the DM state of TKS's model, the monomers are completely free but this is very much peculiar to this model. In our model, since the symmetry of a diamond is broken because $\tilde{J}_3 \neq 1$, the monomer is no longer free and has an effective interaction between neighbouring monomers through the dimer between them. Therefore the DM state of TKS's model is smoothly connected to the spin-fluid state of our model, as can be seen in figure 9. The tetramer in the TD state is also special to TKS's model. When the symmetry of the diamond is broken, the tetramer is decomposed into two dimers existing on stronger bonds, as is shown in figure 5. Then the TD state of TKS's model is a special case of the dimer state of our DD chain model. Thus the physical pictures of our model and TKS's model are consistent with each other.

We can confirm the reliability of our numerical results by checking the properties of excitations. At the SF–dimer critical point, the cosine term of the effective Hamiltonian (3) vanishes and the relation $\Delta E_{\rm ss}(N) = \Delta E_{\rm st}(N)$ holds, as discussed by Okamoto and Nomura [12, 14, 15]. Then the system is purely Gaussian and has low-lying excitation energies proportional to $1/N$ in finite systems. The lowest order correction to $1/N$ may be of $1/N^3$ form. This correction comes from the band curvature and the wavenumber dependence of the coupling constant of the interaction between Jordan–Wigner fermions, which was neglected in the course of deriving the effective Hamiltonian. Figure 14 shows the $1/N^2$ dependence of $N\,\Delta E(N)$ at $\tilde{J}_2 = 1.2$ and $\tilde{J}_3 = 0.39$, which is the SF–dimer critical point where $\Delta E_{\rm ss}(\infty) = \Delta E_{\rm st}(\infty)$. As can be seen from figure 14, the size dependence of the lowest excitation is well expressed as

$$N\,\Delta E(N) = a + (b/N^2) \tag{15}$$

which is consistent with the above-mentioned discussion. The quantity a is related to the spin-wave velocity as

$$a = 2\pi v_{\rm s} x \tag{16}$$

where x is the scaling dimension of this excitation, which is equal to $1/2$ at the critical point [12, 14, 15]. Since $a = 3.851 \pm 0.001$ in the case of figure 14, we obtain

$$v_s = 1.226 \pm 0.001. \tag{17}$$

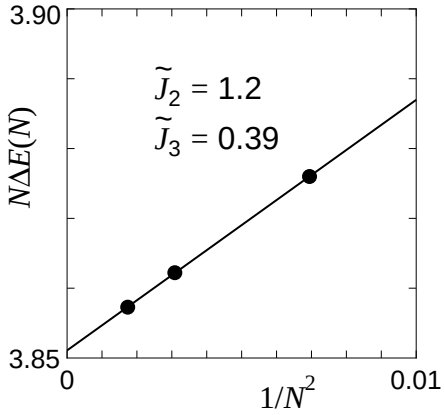

Figure 14. The system-size dependence of the scaled excitation gap $N\,\Delta E$ at the SF–dimer critical point.

The system-size dependence of the ground-state energy also provides us with useful information. Under periodic boundary conditions, it is written as [16, 17]

$$\frac{E_g(N)}{N} = \epsilon_g(\infty) - \frac{\pi v_s c}{6N^2} + \cdots \tag{18}$$

where $E_g(N)$ is the ground-state energy of the N-spin systems, $\epsilon_g(\infty)$ the ground-state energy of the infinite system per spin, v_s the spin-wave velocity and c the conformal charge which is equal to unity in our universality class. Figure 15 shows the system-size dependence of the ground-state energy in the case of $\tilde{J}_2 = 1.2$ and $\tilde{J}_3 = 0.39$. From the slope of the line, we obtain

$$v_s = 1.23 \pm 0.01 \tag{19}$$

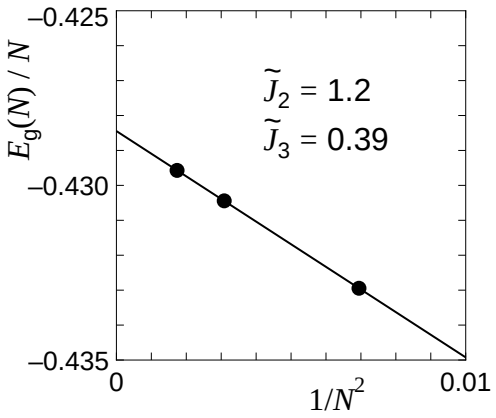

Figure 15. The system-size dependence of the ground-state energy $E_g(N)$ on the SF–dimer critical point.

which agrees well with equation (17). The fact that the values of v_s given by equations (17) and (19) agree within the numerical error justifies our numerical analysis.

The spin-wave velocity v_s can also be obtained from the lowest excitation having $S^z_{tot} = 0$ and $k = 2\pi/N$ from

$$v_s = \lim_{N\to\infty} \frac{N\,\Delta E(N, S^z_{tot} = 0, k = 2\pi/N)}{2\pi}. \tag{20}$$

We note that this formula is free from logarithmic corrections even in the SF region [15]. Figure 16 shows this extrapolation procedure, which leads to $v_s = 1.228 \pm 0.001$. This is also consistent with equation (17) and equation (19).

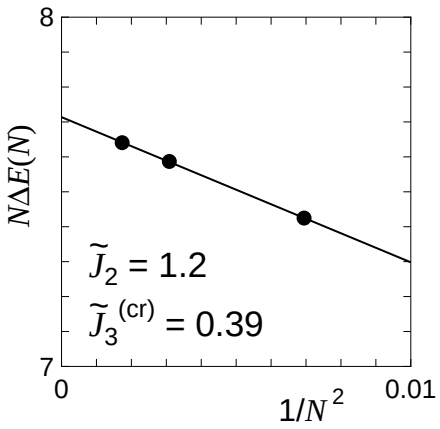

Figure 16. The extrapolation procedure for equation (20). From the intersection, we obtain $v_s = 1.228 \pm 0.001$.

Let us discuss the logarithmic corrections in the SF region. As stated in section 2, there appear logarithmic corrections in various physical quantities when the system is in the SF region. This is very much peculiar to our isotropic case. In the following we check this point numerically. The singlet–singlet gap and the singlet–triplet gap are expressed as

$$\Delta E_{ss}(N) = \frac{2\pi\, v_s x_{ss}}{N} \qquad \Delta E_{st}(N) = \frac{2\pi\, v_s x_{st}}{N} \tag{21}$$

respectively, where x_{ss} and x_{st} are the scaling dimensions:

$$x_{ss} = \frac{1}{2}\left(1 + \frac{3}{2} y_0(N)\right) \qquad x_{st} = \frac{1}{2}\left(1 - \frac{1}{2} y_0(N)\right) \tag{22}$$

with $y_0(N)$ given in equation (10). It is difficult to directly detect the logarithmic dependence in equations (21) and (22) from the numerical data for $\Delta E_{ss}(N)$ and $\Delta E_{st}(N)$. Because the logarithmic corrections are very slowly varying with respect to the system size N, its effects are actually observed as the change in the spin-wave velocity v_s between ΔE_{ss} and ΔE_{st}. As an example, let us take the $\tilde{J}_2 = 1.2$ and $\tilde{J}_3 = 0.35$ point which lies in the SF region. In fact, as shown in figure 17, the spin-wave velocities are estimated to be $v_s = 1.362 \pm 0.001$ and $v_s = 1.248 \pm 0.001$ from ΔE_{ss} and ΔE_{st}, respectively. Okamoto and Nomura [12, 14, 15] used the 'averaged excitation'

$$\Delta E_{ave}(N) = \frac{1}{4}\{\Delta E_{ss}(N) + 3\,\Delta E_{st}(N)\} \tag{23}$$

in which the lowest-order logarithmic corrections vanish, as can be seen from equation (22). From figure 17 we obtain $v_s = 1.277 \pm 0.001$ by use of ΔE_{ave}. When we calculate the

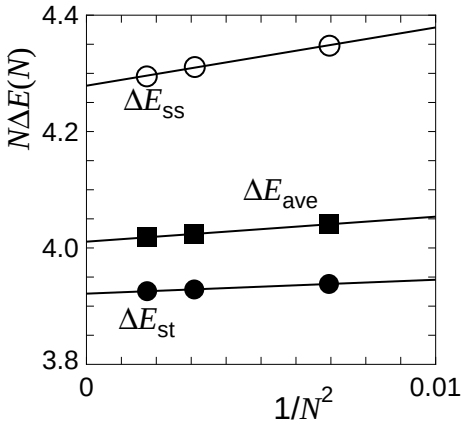

Figure 17. The behaviour of ΔE_{ss}, ΔE_{st} and ΔE_{ave} at the point $(\tilde{J}_2, \tilde{J}_3) = (1.2, 0.35)$ in the SF region. From the intersection of the ΔE_{ave} line, we obtain $v_s = 1.277 \pm 0.001$. The apparent spin-wave velocities are $v_s = 1.362 \pm 0.001$ derived from ΔE_{ss} and $v_s = 1.248 \pm 0.001$ derived from ΔE_{st}.

spin-wave velocity through the formula (20), we obtain $v_s = 1.277 \pm 0.001$, which shows very good agreement with that derived using ΔE_{ave}. We note that there is no logarithmic correction in formula (20), as already stated. Thus our numerical analysis is consistent with our consideration in section 2 with respect to the logarithmic correction, although we could not directly observe its existence. It may need systems with several thousand (or more) spins to directly observe the contribution of the logarithmic corrections.

In summary, we have explained that the frustration leads to the non-magnetic ground state in our DD chain model by use of an analytical method, physical consideration and a numerical method. We have also obtained the phase diagram on the $\tilde{J}_2$–$\tilde{J}_3$ plane numerically.

Acknowledgments

We would like to express our appreciation to H Tanaka for stimulating discussion and also for showing us the experimental results obtained by his group prior to publication. Part of the numerical calculation was done by use of the program package TITPACK Version 2 coded by H Nishimori.

References

[1] Ishii M, Tanaka H, Mori M, Uekusa H, Ohashi Y, Tatani K, Narumi Y and Kindo K 1999 *Preprint*
[2] Swank D D and Willett R D 1974 *Inorg. Chim. Acta* **8** 143
[3] Okamoto K 1992 *Solid State Commun.* **83** 1098
[4] Okamoto K 1996 *Solid State Commun.* **98** 245
[5] Oshikawa M, Yamanaka M and Affleck I 1997 *Phys. Rev. Lett.* **78** 1984
[6] Takano K, Kubo K and Sakamoto H 1996 *J. Phys.: Condens. Matter* **8** 6405
[7] Majumdar C K and Ghosh D K 1969 *J. Math. Phys.* **10** 1399
[8] Majumdar C K 1970 *J. Phys. C: Solid State Phys.* **3** 911
[9] Haldane F D M 1980 *Phys. Rev. Lett.* **45** 1358
[10] Tonegawa T and Harada I 1987 *J. Phys. Soc. Japan* **56** 2153
[11] Kuboki K and Fukuyama H 1987 *J. Phys. Soc. Japan* **56** 3126
[12] Okamoto K and Nomura K 1992 *Phys. Lett.* A **169** 433

[13] Tonegawa T, Harada I and Kaburagi M 1992 *J. Phys. Soc. Japan* **61** 4665
[14] Nomura K and Okamoto K 1993 *J. Phys. Soc. Japan* **62** 1123
[15] Nomura K and Okamoto K 1994 *J. Phys. A: Math. Gen.* **27** 5773
[16] Blöte H W J, Cardy J L and Nightingale M P 1986 *Phys. Rev. Lett.* **56** 742
[17] Affleck I 1986 *Phys. Rev. Lett.* **56** 746